Complete Methods

Animals

The protocols of the present study were designed according to the Guiding Principles in the Care and Use of Animals approved by the Council of the American Physiological Society and were in adherence to the *Guide for the Care and Use of Laboratory Animals* published by the US National Institutes of Health. The study was conducted in adult male Wistar rats (220±20g) and male 8-10 weeks old TRPC3 knockout ($TRPC3^{-/-}$) mice with their age-matched littermate wild-type (WT) controls. Rats were obtained from the "Centre d'Elevage R. Janvier" (Le Genest-Saint Isle, France), whereas mice were developed at Pr Lutz Birnbaumer laboratory at the NIEHS, as previously described (6), and obtained from Pr Nancy Rusch laboratory stock at the University of Arkansas for Medical Sciences. The animals were housed at a stable temperature (25°C) and humidity and were exposed to a 12:12h light-dark cycle. The rats were fed ordinary rat chow, had free access to tap water and were acclimatized for at least one week under these conditions before the start of the study.

Generation of TRPC3 knockout mice

Male 8-10 week old $TRPC3^{-/-}$ mice generated on a 129SvEv/C57BL/6J mixed background and age-matched littermate WT controls were used. $TRPC3^{-/-}$ mice were generated by disrupting the *Trpc3* gene in a three-step process; knockout (KO) and WT mice were genotyped via PCR amplification of the genomic TRPC3 DNA. The genotyping confirmed the omission of exon 7 of the TRPC3 gene in the KO mice as reported by Hartmann et al (6).

Fibroblast isolation and culture

Primary renal fibroblast cultures were prepared as previously described with some modifications (3, 8-10, 12, 16). Animals were anesthetized by ketamine (75mg/kg; Interchemie, Waalre, Holland) and xylazine (10 mg/kg; RotexMedica, Trittau, Germany). Pedal withdrawal reflex was performed to make sure of adequate depth of anaesthesia; when

animals were completely non-responsive to toe pinching, an abdominal incision was performed, kidneys were harvested and rinsed with cold tyrode solution with the following composition (in mM): 117 NaCl, 5.7 KCl, 1.7 $MgCl_2$, 4.4 $NaHCO_3$, 1.5 KH_2PO_4, 10 HEPES, 10 creatine monohydrate, 20 taurine, 11.7 d-glucose, 1% bovine serum albumin, pH 7.1 with NaOH. Kidneys were gently cut into small pieces in tyrode and digested by two oxygenated enzymatic baths (90 rpm shaker at 37°C) for 1 hour. The baths contained each 1 $mg.ml^{-1}$ collagenase A (Roche Diagnostics, Germany) with 1 $mg.ml^{-1}$ bovine serum albumin (Sigma Aldrich, St. Louis, Missouri, USA). Renal tubules were discarded after a first centrifugation (500 rpm, 10 min), then the remaining cells collected after the second one (2000 rpm, 10 min). These remaining cells were put onto a percoll gradient consisting of four different concentrations (40%, 20%, 10% and 5%) and centrifuged at 500 rpm for 20 min. The cell layers obtained in the interface between the 5% and 10% percoll were collected and resuspended in DMEM containing 10% FBS (Lonza, Basel, Switzerland) and 1% penicillin/streptomycin. After 4 hours of culture, the non-adherent cells were removed and medium replenished. Fibroblast counting was done with a haemocytometer to insure that same number of cells was studied in each condition. After 24 hours culture, all cells had the fibroblast characteristic elongated fusiform and spindle shape.

Cell culture treatments

Renal fibroblasts were kept in culture for three days before treatment by the pyrazole-derivative TRPC3 blocker pyr3 (Tocris Bioscience, Bristol, UK) diluted in 100% dimethyl sulfoxide (DMSO) for two days (10µM) as previously described (14, 19, 20, 13). The effect of multiple doses of pyr3 (0.1 µM, 1 µM, 3µM and 10 µM) was also tested on fibroblast proliferation. DMSO (Sigma-Aldrich, St. Louis, Missouri, USA) was used as a vehicle treatment. When ERK inhibitors were used, cells were treated after 3 days of culture for 24 hours with 2-(2-amino-3-methoxyphenyl)-4H-1-benzopyran-4-one (PD98059, 50 µM) or 1,4-

diamino-2,3-dicyano-1,4-bis[2-aminophenylthio]butadiene (U0126, 10 μM). PD98059 and U0126 block ERK 1/2 activation by inhibiting both active and inactive mitogen-activated protein kinase kinase MEK1 and MEK2. PD98059 and U0126 were from Tocris Bioscience, Bristol, UK. Sixteen cultures from 8 rats were performed for each condition. Cell counting was performed under light microscopy.

Ca^{2+} imaging

Cultured renal fibroblasts grown for three days on glass cover-slips were incubated for 45 minutes in serum free DMEM containing 4μM fura-2-am (Molecular Probes, Life Technologies, France) dissolved in DMSO. Cells were washed twice in standard HEPES-buffered saline solution (HBSS) containing (in mM): 135 NaCl; 4 KCl; 1.8 $CaCl_2$; 1 $MgCl_2$; 2.5 HEPES; 10 glucose; pH 7.4 with NaOH. Two perfusion protocols were performed using either diacylglycerol analogue OAG (100 μM) or Ang II (100 nM) (Sigma-Aldrich, St. Louis, Missouri, USA). Nifedipine (1 μM) was used to inhibit the previously reported L-type Ca^{2+} channels (21, 22, 24, 25). Pyr3 was added at a concentration of 10 μM. The non-selective TRPCs blockers SKF96365 (30 μM), gadolinium Gd^{3+} (100 μM), 2-aminoethoxydiphenyl borate (2-APB) (75 μM) were from Sigma. SKF06365 and Gd^{3+} were diluted in ultrapure water while 2-APB in DMSO. Cells were either incubated with the different inhibitors from the start till the end of the recordings, or drugs acutely added after Ca^{2+} entries. Ionomycin (2 μM) and ethylene glycol tetraacetic acid (EGTA 10 mM) were consecutively added at the end of the perfusion protocols in order to check for the maximum and minimum fluorescence values. When Ca^{2+} imaging on siRNA transfected cultures was performed, either transfected cells (tagged cy3-siTRPC1, 3 and 6) or non-transfected cells were analyzed after 48 hours of transfection, with the use of proper fluorescence filters to capture cy3 fluorescence (570 nm). Freshly isolated fibroblasts from sham and UUO kidneys were incubated for 12 hours on glass cover-slips before performing Ca^{2+} recordings. In order to rule out the presence of an

undetermined leak, leak control was performed by incubating the recorded cells in HBSS + or - Ca^{2+} before starting the perfusion protocols.

The ratio of fluorescence (R) excited at the two excitation wavelengths (340/380) was used to estimate intracellular Ca^{2+} concentration ($[Ca^{2+}]i$) as described by Grynkiewicz et al (5): $[Ca^{2+}]i = Kd*(Sf2/Sb2)*[(R-Rmin)/(Rmax -R)]$. Sf2 is the fluorescence measured at 380 nm in Ca^{2+} free solution whereas Sb2 is the fluorescence measured at 380 nm in Ca^{2+} saturating conditions. The dissociation constant for Ca^{2+} binding, *K*d, was estimated to be 224 nM (4, 11, 1, 5, 15). As mentioned above, Rmax was determined from cells dialyzed with 2 µM ionomycin in HBSS containing 1.8 mM $CaCl_2$, whereas Rmin was determined from cells dialyzed with 2 µM ionomycin in Ca^{2+}-free HBSS containing 10 mM EGTA at the end of each experiment.

The manganese quench technique was used to estimate the sarcolemmal permeability to divalent cations. Cells were first perfused with nominally free Ca^{2+} solution, then 50 µM Mn^{2+} was added as a surrogate of Ca^{2+} (quenching solution). The quench rates, before and after application of pyr3, were estimated using linear regression analysis of fluorescence signal and expressed as the percentage of decline per minute (%/min) of the initial fluorescence intensity. Fluorescence quenching measurements were performed at 360 nm (isosbestic point of fura-2) where the fluorescence signal is independent of free calcium concentration.

Emitted fura fluorescence was collected by the 40X objective, passed through a 510 nm filter and detected by a photomultiplier tube. Fluorescence experiments were carried out at room temperature rather than 37 °C, to reduce compartmentalization of fura-2 (18, 7, 23). The calcium and contractility recording system (IonOptix, USA) was used. Data analysis was performed using the ionwizard software (v. 6.1) and sigmaPlot (v. 11.0). Ca^{2+} entry amplitudes were measured by subtracting the ratio values as well as intracellular Ca^{2+} values

just before re-adding Ca^{2+} from those at the Ca^{2+} peak. n=10-14 cells from 4 rats for each condition. Data are represented as mean ± SEM in bar graphs.

Cell proliferation and viability

Cell proliferation assay was done using 3-(4,5-dimethylthiazol-2-yl)-2,5-diphenyltetrazolium bromide (MTT) (Bio Basic Inc, Markham Ontario, Canada). Briefly, same number of cells in each well was grown for three days as previously described, then pyr3 added for two days; afterward, medium was removed and 0.5 $mg.ml^{-1}$ MTT water solution added onto the cells. After 4 hours incubation at 37°C, MTT solution was discarded, then cells washed with PBS. The MTT formazan purple crystals were then dissolved with 100 µl of 100% DMSO, and absorbance read at 550 nm.

Cell viability was assessed by the trypan blue exclusion test. Following the treatments of the cultured cells by pyr3 as previously described, fibroblasts were harvested and labeled with trypan blue (0.4 % in PBS) (Sigma-Aldrich, St. Louis, Missouri, USA) . Trypan blue positive and negative cells were calculated with a haemocytometer. Trypan blue negative cells were regarded as viable cells. The percentage of cell viability was calculated using the following formula: total viable cells (unstained) / total cells (stained and unstained) x 100. H_2O_2 was used on cells at a concentration of 1mM for 4 hours at 37 °C as a positive control in order to induce cell mortality (2, 17).

Sircol collagen assay

Collagen synthesis by fibroblasts was evaluated by the sircol collagen assay (Biocolor, County Antrim, United Kingdom) as described in the manufacturer technical sheet. Briefly, cells were grown and treated with pyr3 as previously described, then medium supernatant collected. Standard curve was performed using collagen from rat tail provided with the assay kit. Sircol dye reagent was added (1 ml) to each sample and standard, then incubated for 30 min. Samples were centrifuged at 12 000 rpm for 10 min, and supernatant discarded. 750 µl

ice-cold acid-salt wash reagent was gently layered on the collagen-dye pellet to remove unbound dye from the surface of the pellet. Samples were then centrifuged at 12 000 rpm for 10 min, tubes drained and 1 ml alkali reagent added to each tube. The bound dye was dissolved with a vortex mixer, and 200 µl of each sample transferred to individual wells of a 96 microwell plate then read at 550 nm. Collagen dosage from tissue of sham and obstructed kidneys was performed as previously described with an additional extraction-concentration step before the ice-cold acid-salt wash: 0.5M acetic acid and pepsin with isolation and concentration reagent (200 µl), overnight at 4°C.

Cell transfection

Cells were transfected with cy3-tagged siRNAs on day 3 and left for 48 hours before assessing TRPC1, 3 and 6 knockout effects. The turbofect transfection reagent (Thermo Scientific, USA) was used according to the manufacturer protocol. siRNA sequences were from Eurogentec (Seraing, Belgium): cy3-siTRPC1 sense 5' CUGCUCAUCGUAACAACUA 3' and antisense 5' UAGUUGUUACGAUGAGCAG 3' ; cy3-siTRPC3 sense 5' CAUUCUCAAUCAGCCAACACGAUAU 3' and antisense 5' AUAUCGUGUUGGCUGAUUGAGAAUG 3' ; cy3-siTRPC6 sense 5' GGACCAGCAUAC AUGUUUA 3' and antisense 5' UAAACAUGUAUGCUGGUCC 3' ; cy3-siScrambled sense 5' AAUACUCGCCCUAAUCCACAGAUAU 3' and antisense 5' AUAUCUGUGGAUUAGGGCGAGUAUU 3'. Transfection efficiency was higher than 90% and was calculated by counting under an epifluorescence microscope the red fluorescent cells that have taken up the siRNAs.

Co-immunoprecipitation and Western blot

Total proteins were extracted from both cultured or freshly isolated renal fibroblasts and renal tissue from rats and mice using a RIPA buffer with protease and phosphatase inhibitors. Protein concentration was determined using the Bradford protein assay (Bio-Rad, France). In

order to perform the immunoprecipitations, five hundred µg of protein were incubated overnight at 4°C in the presence of anti-TRPC1 (20 µg), anti-TRPC3 (20µg), anti-TRPC6 (20µg) or a non-relevant antibody (Rabbit IgG) used as a negative control. Prewashed A/G agarose beads (50 µl) were then added at 4°C for 3 hours. The beads were washed 5 times with lysis buffer and the proteins eluted with 30µl 2X sample loading buffer plus 30µl glycine pH2.5 and heated to 70°C for 10 min. Proteins were separated by SDS 10% PAGE then blotted on Hybond-C membranes (Amersham Biosciences, GE Healthcare, France). Membranes were blocked with either 5% non-fat milk or 5% bovine serum albumin (BSA) and incubated with the various antibodies: anti-TRPC1 1/200, anti-TRPC3 1/200, anti-TRPC6 1/200, anti-p53 1/500, anti-p21 1/500, anti-PCNA 1/1000, anti-Ki67 1/1000, α-SMA 1/1000, total ERK 1/2 1/1000, phospho-ERK 1/500, fibronectin 1/1000, MMP2 1/1000, MMP9 1/1000, TIMP1 1/500. All antibodies were from Abcam, Cambridge, United Kingdom. Visualization was done using enhanced chemiluminescence and developed on Kodak films.

ELISA

ELISA technique was used for quantifying secreted cytokines from cell cultures. TGF-β1, IL1 and IL6 Rat ELISA kits were used according to the manufacturer protocols (Abcam, Cambridge, UK).

Immunocytochemistry

Renal fibroblasts were grown on positively charged glass slides for either 12 hours (day 0 staining) or 5 days (day 5 staining), fixed with 100 % ice-cold ethanol then permeabilized with 0.5 % triton diluted in PBS for 10 min. Blocking was done by 10 % goat serum and cells incubated with primary antibodies overnight at 4°C (Anti-vimentin: 1/250, anti-cytokeratin: 1/250). Primary antibodies were from Abcam, Cambridge, United Kingdom. Biotinylated secondary antibody was added for 1 hour at room temperature, followed by 30 min in 0.6 % hydrogen peroxide. ABC reagent (Vectastain ABC Kit, Vector Laboratories, Inc.,

Burlingame, CA, USA) was then added for 1 hour at room temperature, followed by diaminobenzidine tetrahydrochloride (DAB reagent). Coverslips were mounted with VectaMount (Vector Laboratories, Inc., Burlingame, CA, USA) and visualized under an Olympus sc100 microscope.

Unilateral ureteral obstruction

Animals were anesthetized as previously described. When the rats were completely non-responsive to toe pinching, the left kidney and ureter were exposed via a flank incision. The left ureter was ligated with 4-0 silk at two points and finally the wound was closed. Sham rats underwent the same surgical procedures but the left ureter was left intact. Rats were divided in three groups of 10 each: UUO-DMSO where animals underwent UUO and were treated with DMSO and polyethylene glycol; UUO-pyr3 where animals underwent UUO and were treated with pyr3 (0.1 mg/kg/day; (13)) and sham animals also treated with the same dose of pyr3. Treatments were conducted as previously described (13) by implanting alzet mini-osmotic pumps (Durect, Cupertino, USA) subcutaneously in the back, containing either pyr3 (0.1 mg/kg/day dissolved in 50% DMSO and 50% polyethylene glycol) or vehicle (50% DMSO and 50% polyethylene glycol). Osmotic pumps were implanted 3 days before UUO and kept till sacrifice at day 10 in order to assure a complete block of TRPC3 from the beginning till the end of the experiments.

Similarly, UUO was conducted on mice; animals were divided in four groups of 8 each: UUO-WT, UUO-TRPC3$^{-/-}$, sham WT and sham TRPC3$^{-/-}$. Sacrifice was also done on day 10 after surgery.

Renal tissue preparation for histopathology

The animals (rats and mice) were anesthetized as previously mentioned, then the left kidneys excised. Kidneys were perfused with a ringer solution until all blood was removed, then de-capsulated, cut into half through a mid-sagittal plane and one half fixed with 10% formalin

solution (Sigma-Aldrich, St. Louis, Missouri, USA); whereas the other half dissected into 3 pieces destined for fibroblast cell isolation as well as RNA and protein extractions. The formalin-fixed tissue was embedded in paraffin and sections of 4 µm thickness were cut. Paraffin-embedded sections of the kidneys were stained with either hematoxylin eosin or Masson's trichrome (Sigma-Aldrich, St. Louis, Missouri, USA) for histopathological evaluation. Mice kidneys were further stained with picrosirius red (Sigma-Aldrich, St. Louis, Missouri, USA). After staining, the sections were rinsed in distilled water, dehydrated in ethanol/water baths with decreasing water content, and finally rinsed in xylene before being mounted with a permanent mounting medium. Antibodies for α-SMA were from BioGenex, CA, USA and TRPC3 from Abcam, Cambridge, UK. Antigen retrieval was performed in a microwave for TRPC3 labeling. Gross examination and histological sections were analyzed by two independent pathologists in a blinded fashion. A semi-quantitative scoring system was used to assess interstitial changes such as inflammation and fibrosis. Interstitial inflammation refers to the presence of aggregates of leukocytes in the interstitium. Fibrosis analysis was done with the ImageJ program, by thresholding the acquired pictures, then creating selections of the fibrotic areas. Six sections were analyzed for each rat and mouse.

Gene quantifications

Total RNA was extracted from the previously treated cultured renal fibroblasts, as well as the freshly isolated cells from sham and UUO kidneys (rats and mice) by the use of trizol (Life Technologies, Carlsbad, California, USA). Samples were then purified with ethanol 75% and purity and concentration of RNA determined by measuring the absorbance at 260 nm with the nanodrop spectrophotometer ND-1000 (Thermo Scientific, Wilmington, Delaware, USA). cDNA was synthesized using random primers (250 ng/µl), dNTP (10 mmol/l) and the superscript III reverse transcriptase kit (Life Technologies, Carlsbad, California, USA). Real time PCR was conducted using the 7500 real time PCR system and the Sybr green PCR

master mix (Life Technologies, Carlsbad, California, USA). Samples were run in triplicates. Melting curves were performed at the end of the amplification to confirm the specificity of the amplified products. In addition, 'no RT' control reactions were done by omitting the reverse transcriptase to confirm the absence of contaminating genomic DNA. Glyceraldehyde 3-phosphate dehydrogenase (GAPDH) was used as a housekeeping gene, and quantifications conducted using the $2^{\Delta\Delta Ct}$ method. The primers (Eurogentec, Seraing, Belgium) used are presented in supplemental table 1.

Statistical analysis

All quantitative data are reported as means ± SEM. Statistical analysis was performed with the SigmaPlot (v11.0) software. One-way ANOVA tests were performed for multiple comparisons of values. Post-hoc two tailed t test comparisons were performed to identify which group differences accounted for significant overall ANOVA results. All values with $p<0.05$ were considered significant.

References

1. Borzak, S, Kelly, RA, Kramer, BK, Matoba, Y, Marsh, JD & Reers, M: In situ calibration of fura-2 and BCECF fluorescence in adult rat ventricular myocytes. *Am J Physiol,* 259**:** H973-81, 1990.
2. Cerella, C, Coppola, S, Maresca, V, De Nicola, M, Radogna, F & Ghibelli, L: Multiple mechanisms for hydrogen peroxide-induced apoptosis. *Ann N Y Acad Sci,* 1171**:** 559-63, 2009.
3. Fu, P, Liu, F, Su, S, Wang, W, Huang, XR, Entman, ML, Schwartz, RJ, Wei, L & Lan, HY: Signaling mechanism of renal fibrosis in unilateral ureteral obstructive kidney disease in ROCK1 knockout mice. *J Am Soc Nephrol,* 17**:** 3105-14, 2006.
4. Gailly, P, Boland, B, Himpens, B, Casteels, R & Gillis, JM: Critical evaluation of cytosolic calcium determination in resting muscle fibres from normal and dystrophic (mdx) mice. *Cell Calcium,* 14**:** 473-83, 1993.
5. Grynkiewicz, G, Poenie, M & Tsien, RY: A new generation of Ca2+ indicators with greatly improved fluorescence properties. *J Biol Chem,* 260**:** 3440-50, 1985.
6. Hartmann, J, Dragicevic, E, Adelsberger, H, Henning, HA, Sumser, M, Abramowitz, J, Blum, R, Dietrich, A, Freichel, M, Flockerzi, V, Birnbaumer, L & Konnerth, A: TRPC3 channels are required for synaptic transmission and motor coordination. *Neuron,* 59**:** 392-8, 2008.
7. Hopf, FW, Turner, PR, Denetclaw, WF, Jr., Reddy, P & Steinhardt, RA: A critical evaluation of resting intracellular free calcium regulation in dystrophic mdx muscle. *Am J Physiol,* 271**:** C1325-39, 1996.
8. Johnson, DW, Saunders, HJ, Baxter, RC, Field, MJ & Pollock, CA: Paracrine stimulation of human renal fibroblasts by proximal tubule cells. *Kidney Int,* 54**:** 747-57, 1998.
9. Johnson, DW, Saunders, HJ, Brew, BK, Ganesan, A, Baxter, RC, Poronnik, P, Cook, DI, Gyory, AZ, Field, MJ & Pollock, CA: Human renal fibroblasts modulate proximal tubule cell growth and transport via the IGF-I axis. *Kidney Int,* 52**:** 1486-96, 1997.
10. Johnson, DW, Saunders, HJ, Johnson, FJ, Huq, SO, Field, MJ & Pollock, CA: Cyclosporin exerts a direct fibrogenic effect on human tubulointerstitial cells: roles of insulin-like growth factor I, transforming growth factor beta1, and platelet-derived growth factor. *J Pharmacol Exp Ther,* 289**:** 535-42, 1999.
11. Kajita, J & Yamaguchi, H: Calcium mobilization by muscarinic cholinergic stimulation in bovine single airway smooth muscle. *Am J Physiol,* 264**:** L496-503, 1993.
12. Kelynack, KJ, Hewitson, TD, Nicholls, KM, Darby, IA & Becker, GJ: Human renal fibroblast contraction of collagen I lattices is an integrin-mediated process. *Nephrol Dial Transplant,* 15**:** 1766-72, 2000.
13. Kiyonaka, S, Kato, K, Nishida, M, Mio, K, Numaga, T, Sawaguchi, Y, Yoshida, T, Wakamori, M, Mori, E, Numata, T, Ishii, M, Takemoto, H, Ojida, A, Watanabe, K, Uemura, A, Kurose, H, Morii, T, Kobayashi, T, Sato, Y, Sato, C, Hamachi, I & Mori, Y: Selective and direct inhibition of TRPC3 channels underlies biological activities of a pyrazole compound. *Proc Natl Acad Sci U S A,* 106**:** 5400-5, 2009.
14. Koenig, S, Schernthaner, M, Maechler, H, Kappe, CO, Glasnov, TN, Hoefler, G, Braune, M, Wittchow, E & Groschner, K: A TRPC3 blocker, ethyl-1-(4-(2,3,3-trichloroacrylamide)phenyl)-5-(trifluoromethyl)-1H-pyrazole-4-c arboxylate (Pyr3), prevents stent-induced arterial remodeling. *J Pharmacol Exp Ther,* 344**:** 33-40, 2013.
15. Malgaroli, A, Milani, D, Meldolesi, J & Pozzan, T: Fura-2 measurement of cytosolic free Ca2+ in monolayers and suspensions of various types of animal cells. *J Cell Biol,* 105**:** 2145-55, 1987.

16. Masterson, R, Hewitson, TD, Kelynack, K, Martic, M, Parry, L, Bathgate, R, Darby, I & Becker, G: Relaxin down-regulates renal fibroblast function and promotes matrix remodelling in vitro. *Nephrol Dial Transplant,* 19**:** 544-52, 2004.
17. McKeague, AL, Wilson, DJ & Nelson, J: Staurosporine-induced apoptosis and hydrogen peroxide-induced necrosis in two human breast cell lines. *Br J Cancer,* 88**:** 125-31, 2003.
18. Negulescu, PA & Machen, TE: Intracellular ion activities and membrane transport in parietal cells measured with fluorescent dyes. *Methods Enzymol,* 192**:** 38-81, 1990.
19. Sabourin, J, Antigny, F, Robin, E, Frieden, M & Raddatz, E: Activation of transient receptor potential canonical 3 (TRPC3)-mediated Ca2+ entry by A1 adenosine receptor in cardiomyocytes disturbs atrioventricular conduction. *J Biol Chem,* 287**:** 26688-701, 2012.
20. Sabourin, J, Robin, E & Raddatz, E: A key role of TRPC channels in the regulation of electromechanical activity of the developing heart. *Cardiovasc Res,* 92**:** 226-36, 2011.
21. Shivakumar, K & Kumaran, C: L-type calcium channel blockers and EGTA enhance superoxide production in cardiac fibroblasts. *J Mol Cell Cardiol,* 33**:** 373-7, 2001.
22. Soldatov, NM: Molecular diversity of L-type Ca2+ channel transcripts in human fibroblasts. *Proc Natl Acad Sci U S A,* 89**:** 4628-32, 1992.
23. Takahashi, A, Camacho, P, Lechleiter, JD & Herman, B: Measurement of intracellular calcium. *Physiol Rev,* 79**:** 1089-125, 1999.
24. Yang, S & Huang, XY: Ca2+ influx through L-type Ca2+ channels controls the trailing tail contraction in growth factor-induced fibroblast cell migration. *J Biol Chem,* 280**:** 27130-7, 2005.
25. Zhu, DL, Herembert, T, Caruelle, D, Caruelle, JP & Marche, P: Involvement of calcium channels in fibroblast growth factor-induced activation of arterial cells in spontaneously hypertensive rats. *J Cardiovasc Pharmacol,* 23**:** 395-400, 1994.

Supplemental data

Supplemental Table 1: Forward and reverse primers used for quantitative real time PCR.

	Rat primers	
Gene	**Forward primer (5'-3')**	**Reverse primer (5'-3')**
Trpc1	AGCCTCTTGACAAACGAGGA	ACCTGACATCTGTCCGAACC
Trpc2	TTGCTGGGAGAGTCTCTGGT	CCTCGATCCACACCTCCTTA
Trpc3	GAGATCTGGAATCGGTGGAA	AAAAGCTGCTGTTGGCAGTT
Trpc4	GACACGGAGTTCCAGAGAGC	GTTGGGCTGAGCAACAAACT
Trpc5	CCGCAAGGAGGTGGTAGG	TGTGATGTCTGGTGTGAACTC
Trpc6	TACTGGTGTGCTCCTTGCAG	GAGCTTGGTGCCTTCAAATC
Trpc7	AACGAGACCTTCACAGACTAC	GCATTCAGACCAGATCATTCC
Col1	CTGGCGCAAGAGGCGAGAGA	AGCTCCGGGGGCACCAGTAT
Col3	AAACGGAGAACGGGGTGGCC	TCACCAGGTGCGCCAGTAGGT
Col4	AGTCGGTCCCATCGGTCCCA	AGCCTCGGTCACCTTGTGGC
IL1	CTGACAGACCCCAAAAGATTAAGG	CCTTGTCGAGATGCTGCTGTGA
IL6	TCCGCAAGAGACTTCCAGCCA	AAGCCTCCGACTTGTGAAGTGGT
MMP2	TGCAGGGTGGTGGTCACAGC	AGCTCAGCAGCCCAGCCAGT
MMP9	GCGTGTACGGGCTCGAAGCA	AGTAAGTGGGGACCACGGCG
Fn1	CGCCGAGCATTCTGCCGGAA	TCGGAAACCGTGGATTGCTGGC
TIMP1	TTTCCGGTTCGCCTACACCCC	TCCTTAAACGGCCCGCGATGAG
TGF-β1	ATGGTGGACCGCAACAACGCAATC	CACGGGACAGCAATGGGGGTT
MCP1	CAGCCAGATGCAGTTAATGCCCC	GCTTCTTTGGGACACCTGCTGCTG
cTGF	TGTGCACGGAGCGTGATCCC	TGCACCATCTTTGGCAGTGCACA
Cox2	CAGACAGATTGCTGGCCGGGTTG	TCAGGGAGAAGCGTTTGCGGT
Alox5	GCGGGCACCGACGACTACAT	ACGTCATAGGAGTCGCGACCGC
CD31	GTGGAAGACCCGAGACTGAG	GAGGTATCGAATGGGCAGAA
Cadherin 16	GCCAAGACTACGGTGTGGTT	AGGTAGGCGTGGGAATCATTG
EpCAM	GGCTGAGATAAAGGAGATGGGT	ATCCTCCCCAGGTCTATCCG
E-cadherin	GGCATCACCACAGAGACCC	CGCCCTTTTGATTTTCCGGG
CD68	TGTACCTGACCCAGGGTGGAA	GAATCCAAAGGTAAGCTGTCCGTAA
CD11c	TCAGCAGCCACGACCAATTT	CCACACCGTTTCTCCCTTCA
FAP	TCCACGGAACAGCAGATGAT	GTCAGAGTACCACATCGCCT
ACTB	CGTGAAAAGATGACCCAGATCA	TGGATGGCTACGTACATGGC
TBP	CCACACCAGCCTCTGAGAGC	ATACAATATTTTGGAGCTGTGGTACAA
RPL32	CCAGAGGCATCGACAACA	GCACTTCCAGCTCCTTGACAT
GAPDH	GGCTCTCTGCTCCTCCCTGTTCTA	GCCAAATCCGTTCACACCGACCT
	Mouse primers	
Gene	**Forward primer (5'-3')**	**Reverse primer (5'-3')**
Ki67	TGAATCTGTGGAAGAGCAGGTT	TTCGGTACCTAGAGTTCTGATCTGG
PCNA	GGGTGAAGTTTTCTGCAAGTGG	CATTCATCTCTATGGTTACCGCC
α-SMA	GACAGAGGCACCACTGAAC	GAGTCCAGCACAATACCAGTTG
TGF-β1	AGAGCGCCGACCCAGA	TGGTTTTCTCATAGATGGCGTTG
cTGF	CCCTAGCTGCCTACCGACTG	TTAGAACAGGCGCTCCACTC
IL1	TGCCACCTTTTGACAGTGATG	ATGTGCTGCTGCGAGATTTG
IL6	CCGGAGAGGAGACTTCACAG	GCCATTGCACAACTCTTTTCTC
MCP1	CACTCACCTGCTGCTACTCA	GCTTGGTGACAAAAACTACAGC
GAPDH	GGAGAGTGTTTCCTCGTCCC	ATGAAGGGGTCGTTGATGGC

Abbreviations: Trpc1-7: Transient receptor potential canonical 1-7; Col1: Collagen 1; Col3: Collagen 3; Col4: Collagen 4; IL1: Interleukin 1; IL6: Interleukin 6; MMP2: Matrix metalloproteinase 2; MMP9: Matrix metalloproteinase 9; Fn1: Fibronectin 1; TIMP1: Tissue inhibitor of metalloproteinases 1; TGF-β1: Transforming growth factor beta 1; MCP1: Monocyte chemoattractant protein 1; cTGF: Connective tissue growth factor; Cox2: Cyclooxygenase 2; Alox5: Arachidonate 5-lipoxygenase; EpCAM: epithelial cell adhesion molecule ; CD31, CD68 and CD11c: clusters of differentiation 31, 68 and 11c; FAP: fibroblast activation protein; ACTB: beta actin; TBP: tata box protein; RPL32: ribosomal protein L32; PCNA: proliferating cell nuclear antigen; GAPDH: Glyceraldehyde 3-phosphate dehydrogenase.

Supplemental Figure 1: Characterization of cation influx in cultured rat renal fibroblasts by Mn^{2+} quenching experiments. Representative recordings (**A-C**) and quantifications (**D**) of fura-2 fluorescence during perfusion with 50 µM Mn^{2+} and stimulation with either OAG or Ang II, showing the chronic and acute effects of TRPC3 blockade with pyr3 on cation influx. Ionomycin was added at the end of each protocol to assess the maximum quenching percentage. Entry of Mn^{2+} into cytoplasm was monitored by fluorescence quenching measurements at 360 nm in fura-2 loaded cells. Measurements are expressed as the percentage of decline per minute (%/min) of the initial fluorescence intensity. n=10-14 cells from 4 rats for each condition. Data for fura-2 amplitudes are represented as mean percentage of control ± SEM. *p<0.01 *vs* control.

Supplemental Figure 2: TRPC3 blockade does not affect basal Ca^{2+} entry in cultured rat renal fibroblasts. **A**, **B**: Representative recordings and quantifications of fura-2 emission ratio (ΔF340/F380) showing the absence of a detectable basal Ca^{2+} entry after the on-off Ca^{2+} switch. Pyr3 did not have any noticeable effect. **C, D**: Representative recordings (at 360, 340

and 380 nm excitations and 510 emissions) and quantifications of fura-2 emission ratio (ΔF340/F380) in renal fibroblasts after consecutive addition of ionomycin (2 µM) and 10 mM EGTA to evaluate the maximum and minimum fura-2 ratio values. n=10-14 cells from 4 rats for each condition. Data for fura-2 amplitudes are represented as mean percentage of control ± SEM.

Supplemental Figure 3: Stability of fura-2 signal in the studied rat renal fibroblasts. Basal fura-2 emission at 360 nm was assessed over time after loading the cells with fura-2-am without any stimulation. Stable fluorescence ruled out a significant fura-2 leak from the cells. n=10-14 cells from 4 rats for each condition. Data for fura-2 amplitudes are represented as mean percentage of control ± SEM.

Supplemental Figure 4: High purity of rat renal fibroblast cell culture preparations. Immunocytochemistry revealing positive vimentin (**A, C**), and negative cytokeratin expressions (**B, D**) in the cultured rat renal fibroblasts at day 0 and day 5 respectively. **E**: Quantification of either vimentin or cytokeratin positively marked cells at days 0 and 5 of culture. **F**: Expression of endothelial (CD31), epithelial (Cadherin 16, EpCAM, E-cadherin), monoytes/macrophages (CD68) and dendritic cells (CD11c) markers in the rat renal cell culture preparations at days 0 and 5. Total rat kidney mRNA was used as a positive control. Studied genes were normalized to GAPDH. Magnifications: x100 (**A-D left panels**) and x400 (**A-D right panels**). Scale bars: 50 and 12 µm for left and right panels respectively. n=16 cultures from 8 rats for each condition. a.u.: Arbitrary units. Data are represented as mean ± SEM. *p<0.001 *vs* vimentin and cell cultures.

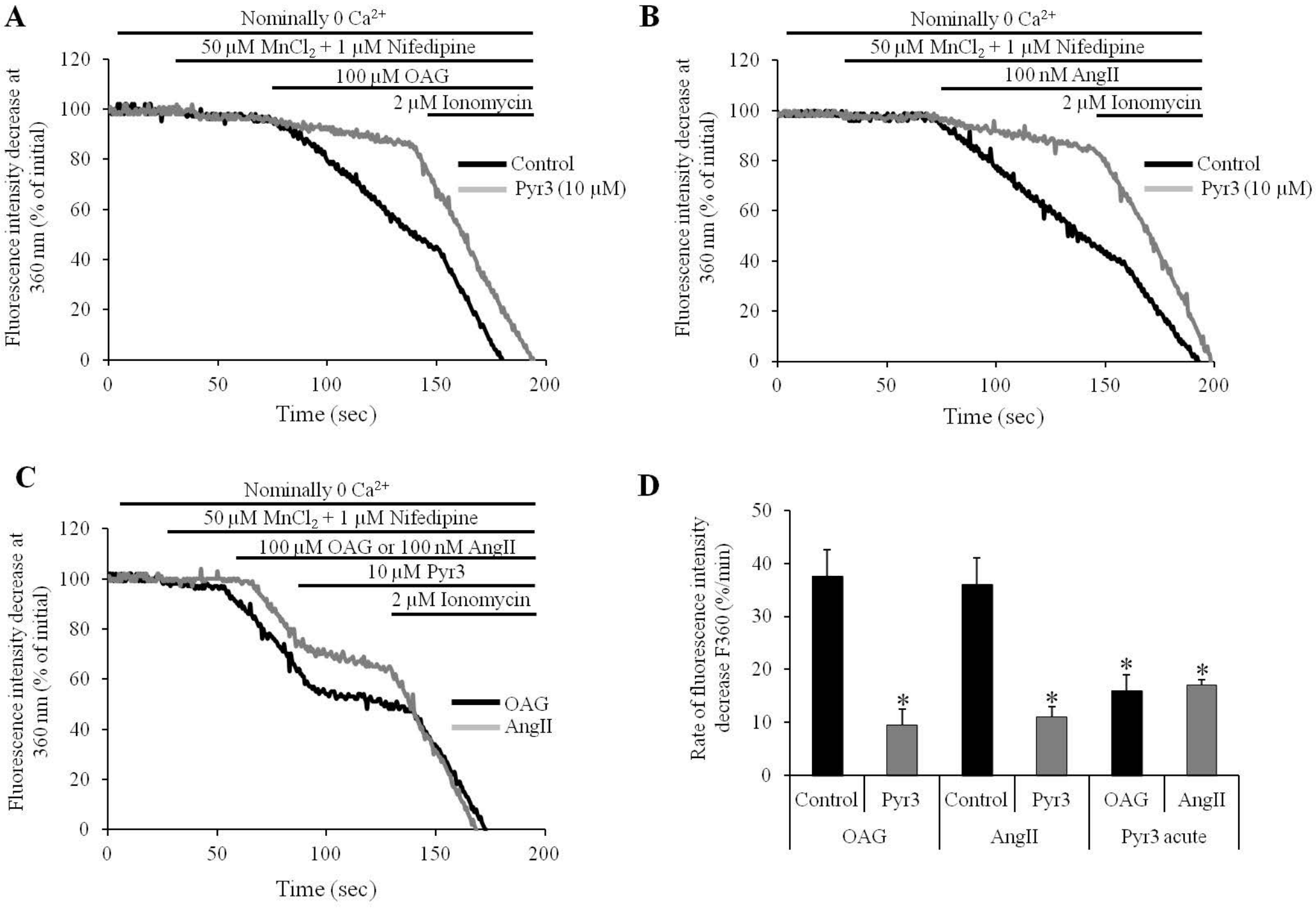

Supplemental Figure 1

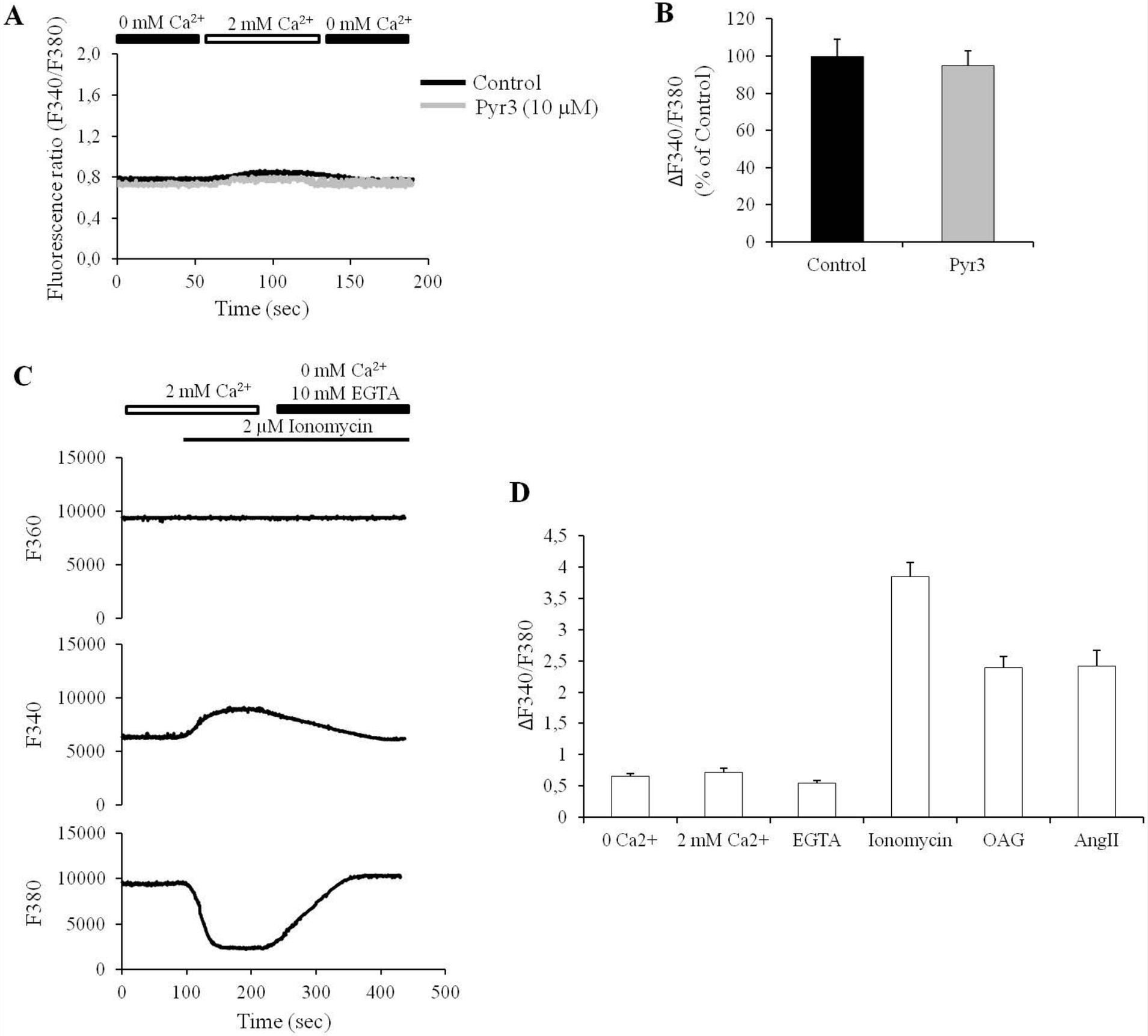

Supplemental Figure 2

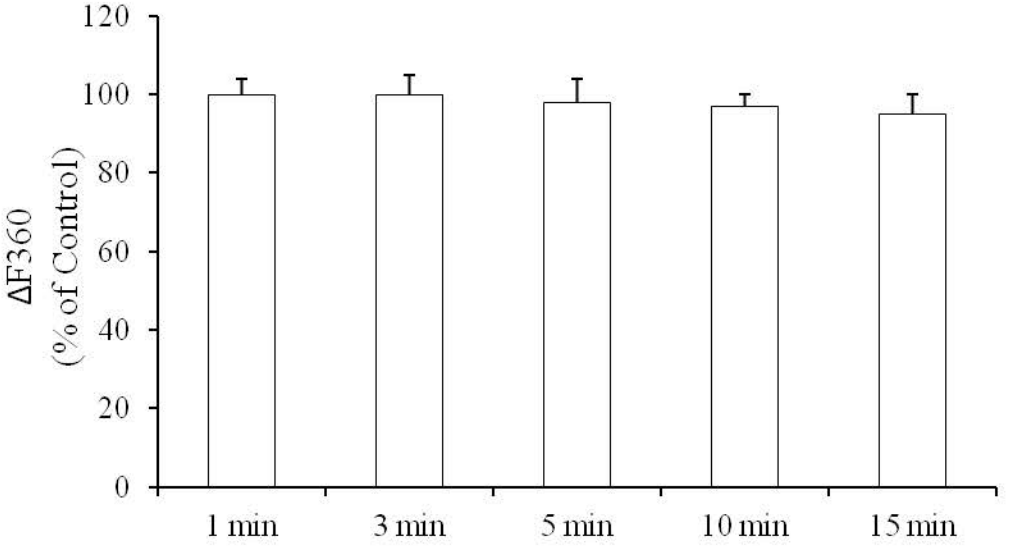

Supplemental Figure 3

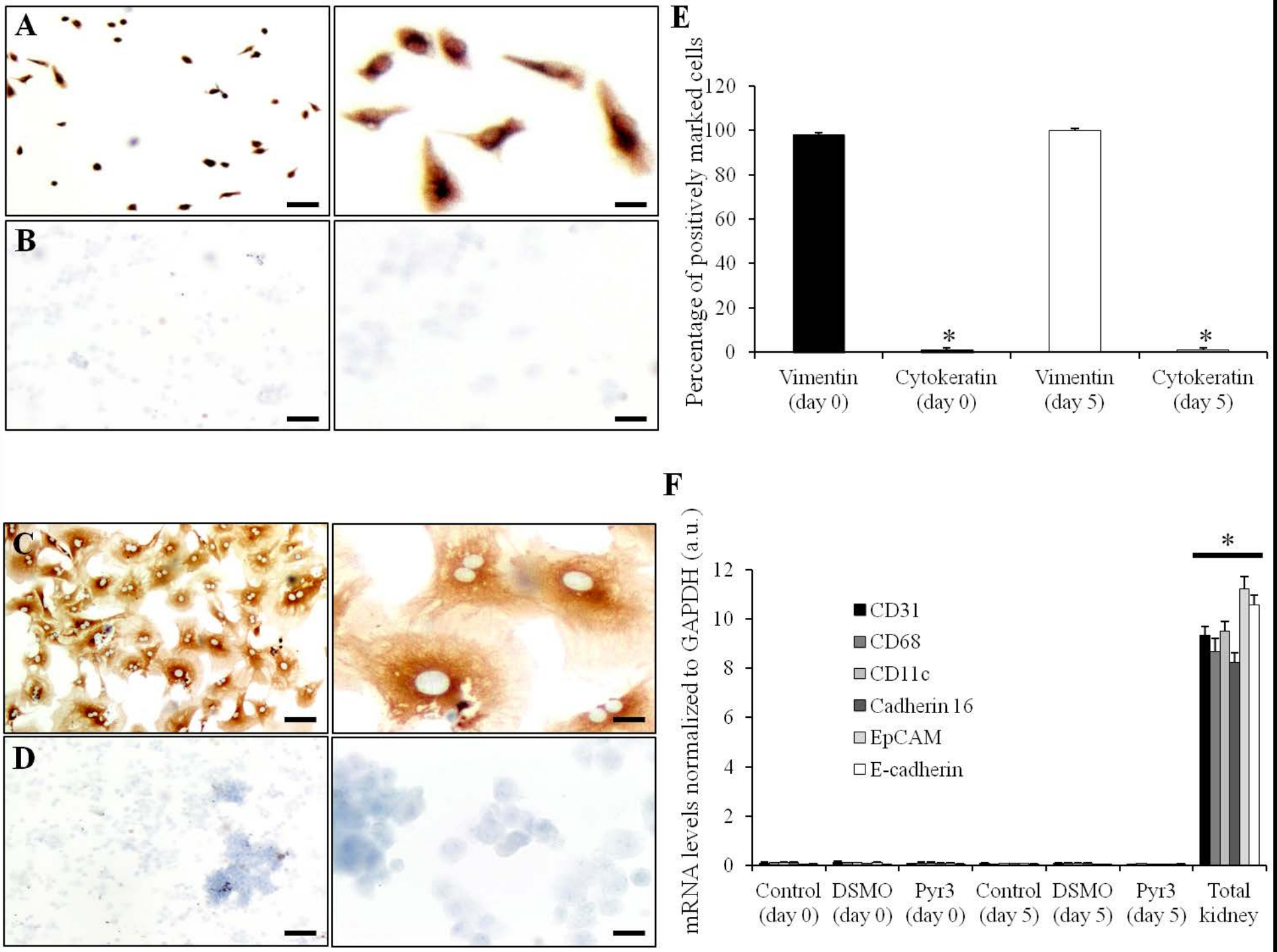

Supplemental Figure 4